



Research Paper

Influence of Sodium Tripolyphosphate Concentration on Characteristics and Performance of Polyamide Thin Layer Membrane in Cu (II) Removal

Yaghoub Mansourpanah*, Parivash M. Rashnou

Membrane Research Laboratory, Lorestan University, Khorramabad, P.O. Box 68137-17133, Iran

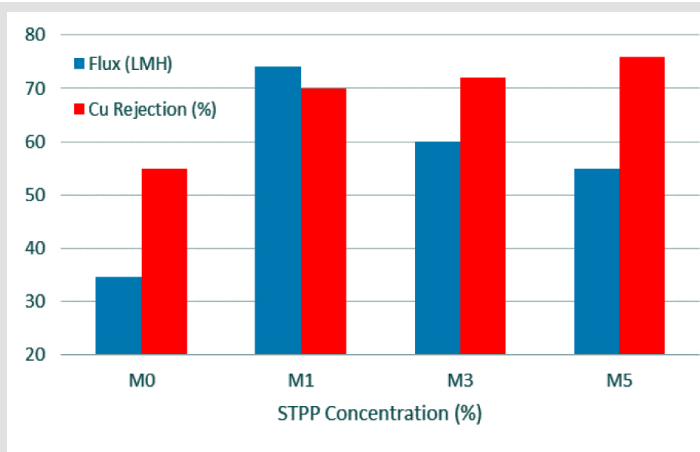
ARTICLE INFO

Received 2016-02-10
 Revised 2016-05-16
 Accepted 2016-05-21
 Available online 2016-05-21

KEYWORDS

PA thin layer
 Inorganic salt
 STPP
 Morphology

GRAPHICAL ABSTRACT



HIGHLIGHTS

- Increasing the Cu²⁺ rejection capability of the membranes with loading STPP
- Formation of a dense and compacted surface in the presence of STPP
- Increasing the flux and antifouling properties of the thin film membranes
- Slight changes in the chemical structure of the thin layers

ABSTRACT

In this work, the effect of presence of the sodium tripolyphosphate (STPP), as an inorganic salt, on improving the performance of polyamide (PA) thin layer membranes has been studied. Characterization analyses confirmed the presence of the salt on the whole surface structure of the thin layer. Different salt loadings resulted in different fluxes and Cu (II) rejections. The thin layer containing 1% w/w STPP showed favorable flux and relatively good rejection for the Cu²⁺ ions. However, the best rejection was obtained for 5% w/w STPP. Atomic force microscopy (AFM) and scanning electron microscopy (SEM) images confirmed the formation of a dense and compact surface in the presence of STPP in the aqueous phase.

© 2017 MPRL. All rights reserved.

1. Introduction

Structurally, most NF membranes are thin film composites (TFC) with a selective layer above a porous support. Thin film composite membranes show several advantages such as low operation pressure, high permeate flux, high retention of multivalent ions, and separation of compounds with different molecular weights [1, 2]. Among different fabricating methods of the thin film membranes including plasma-initiated polymerization, photo-initiated polymerization, coating, and interfacial polymerization, the latter procedure has attracted more attention compared to others [3-5]. This technique is based

on a poly condensation polymerization reaction between an amine functional group in the aqueous phase (e.g. PIP) and an insoluble acid chloride functional group in the organic phase (e.g. TMC) [6, 7]. These types of membranes have been used in many applications including wastewater treatment, industrial water production, water softening, pharmaceutical, textile, and chemicals processing.

To develop new TFC membranes, many studies have focused on both synthesis of new monomers with special functional groups and adding effective additives in the membrane matrix [8, 9].

* Corresponding author at: Phone: +98 66 33120611, fax: +98 66 33120612
 E-mail address: mansourpanah.y@lu.ac.ir; jmansourpanah@yahoo.com (Y. Mansourpanah)

The proposed additives can be inorganic salts [10, 11], surfactants [2], and/or polymers [12-14]. Addition of additives can change and modify the surface and bulk structures of thin film composites which induce remarkable changes in separation performance and surface chemistry including changing the hydrophilicity, affecting the diffusion rate of monomers into different phases, compressing the surface, and etc. [2].

Major attempts were made to improve the water flux of TFC membranes by adding different additives in two immiscible phases without notable decrease of salt rejection. Jin et al. showed that the addition of nano-SiO₂ into the polyamide thin layer improved the thermal stability, hydrophilicity and the permeation properties [10]. Mansourpanah et al. studied the effect of TiO₂ nanoparticles on skin layer structure which showed notable hydrophilicity and outstanding anti-fouling properties [11]. In another work, Lind et al. investigated the presence of three different-sized zeolite crystals in the structure of reverse osmosis polyamide thin layer membranes which induced significant changes in the structure, morphology, charge, hydrophilicity, and separation performances of the membranes [15].

In this study, several TFC polyamide membranes were fabricated using the interfacial polymerization technique and loading different concentrations of the sodium tripolyphosphate (STPP) in the aqueous phase. The STPP is an inorganic compound with formula Na₅P₃O₁₀ (Figure 1). It is the sodium salt of the polyphosphate penta-anion, which is the conjugate base of the triphosphoric acid. It is produced in large scale and is used as a component for many domestic and industrial products, especially detergents. The effects of the mentioned salt on the performance, morphology and physicochemical properties of the prepared membranes were investigated.

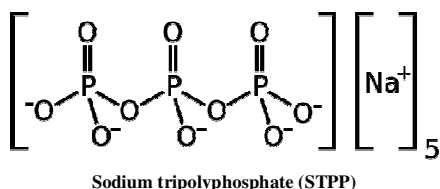


Fig. 1. The chemical structure of the STPP salt.

2. Experimental

2.1. Materials

Polyethersulfone (PES Ultrason E6020P with $M_w=58,000$ g/mol) was supplied from the BASF (Germany). *N,N*-dimethylformamide (DMF) and trimesoyl chloride (TMC) were purchased from the Sigma Aldrich. Piperazine (PIP), triethylamine (TEA), poly (ethylene glycol) 600 (PEG 600), acrylic acid (AA), CuSO₄ and *n*-hexane were purchased from the Merck. Bovine serum albumin (BSA) powder (assay > 96%, mol wt.; 66 kDa, pH ≈ 7, solubility > 40 mg/mL in H₂O) was obtained from the Sigma. Distilled water was used throughout this study.

2.2. Preparation of the PES support

By dissolving 18 % w/w PES in a mixture of the dimethylformamide (DMF), 5 % w/w of the PEG 600 and 3 % w/w of the acrylic acid, the casting solution was prepared which was then stirred for 5 h at 50 °C at 300 rpm. The dope solution was kept at ambient temperature for about 24 h to remove all air bubbles and obtain a homogeneous solution. Furthermore, the prepared dope solution was cast on a non-woven polyester film (with 150 mm thickness) at 150 μm height using a film applicator at room temperature without evaporation. After coating step, the support was immersed and held in a distilled water bath for at least 24 h to remove most of the solvent and water-soluble polymer.

2.3. Preparation of the thin-film composite membranes

Thin film composite (TFC) membranes were fabricated by the interfacial polymerization technique. In the first step, the aqueous phase solution was prepared by dissolving 0.15% w/w of PIP and 0.4% w/w of TEA in water (composed of 1, 3, and 5% w/w inorganic salt), while the organic phase solution was obtained by dissolving 0.1% w/w of TMC in an organic solvent (i.e. *n*-hexane). Then, the PES supporting membrane was fixed between two Teflon frames with 0.7cm height and 7.5 cm × 20 cm inner cavity. Afterwards, the aqueous phase was poured on the upper surface of the PES membrane and was allowed to soak for at least 10 min. The surface was rolled with a soft rubber roller to remove any small bubbles formed during

immersion. After replacing the aqueous phase, the organic solution was poured on the top of the support membrane for 5 min. At the end, the membrane samples were washed with distilled water and dried at room temperature. The composition of the thin layers is summarized in Table 1.

Table 1. The composition of the prepared thin layers.

Membrane	STPP (% w/w)
PES support-Ms	-
Thin Layer-M0	0
Thin Layer-M1	1
Thin Layer-M3	3
Thin Layer-M5	5

2.4. Characterization of the membrane samples

To study the morphological features of the membranes' modified thin layer at the presence of STPP, a field emission-scanning electron microscope (MIRA3, TESCAN) was employed. First, each sample's surface was perfectly cleaned and then the membrane samples were sputtered by the gold. The coated samples were then observed at 25kV.

An atomic force microscope (DME model C-21, Denmark, Series DS-95) was used to determine the nonstructural surface characteristics and roughness of the thin layer. A small square piece of the prepared membranes was glued on a glass substrate and then the membrane surfaces were observed and analyzed in a scan size of 1 μm × 1 μm.

An FT-IR spectrometer (Equinox 55 Bruker, Germany) with an attenuated total reflection (ATR) attachment was employed to determine the chemical alterations of the membranes' thin layer. Totally, 32 scans were measured during IR study for each sample. The resolution of the apparatus was 4 cm⁻¹.

In order to measure the surface hydrophilicity of the prepared thin layers, a contact angle system (G10, KRUSS; Germany) was employed to measure the static contact angle. Deionized water was used as the probe liquid in all measurements. To minimize the experimental error, the contact angle was measured at five random locations for each sample and the average values are reported.

The performances of the prepared membranes were analyzed using a dead-end filtration system, including a 100ml stirring filtration cell under 0.8MPa. The membrane surface area in the filtration cell was 12.56cm² and the required pressure was supplied by a nitrogen gas cylinder. The permeate solution was collected and weighted by an analytical balance. Ion rejection capability was measured by detecting the permeate conductivity using a conductivity-meter (Hanna 8733 Model, Italy). Salt rejection was determined for all membranes by equation (1) using 1000 ppm CuSO₄ solutions:

$$R\%_{\text{salt}} = \left[1 - \frac{\lambda_p}{\lambda_f} \right] \times 100 \quad (1)$$

where λ_p and λ_f are ion conductivities in the permeate and the feed solutions, respectively.

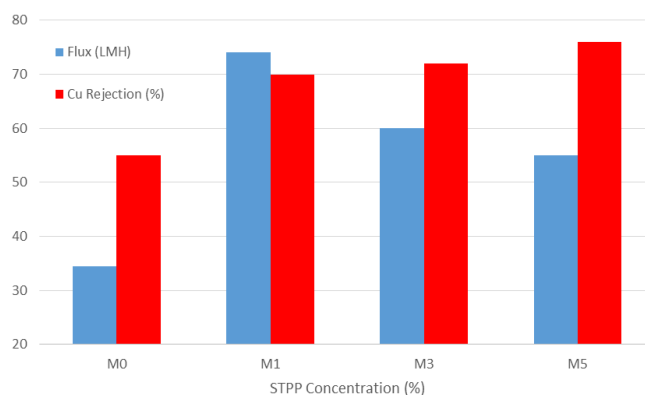


Fig. 2. Flux and Cu²⁺ ion rejection capability of the thin layer membranes.

In order to investigate the antifouling properties of the thin layer, a BSA solution was utilized as a foulant model. During the filtration experiments, a resistance could appear on the surface which could reduce the membrane performance. The resistance was due to the formation of a cake or gel layer on the membrane surface. The strength of the obtained membranes against fouling could be determined by removing this resistance. For each membrane the permeate samples were collected over a certain time period and were then weighted. First, the pure water flux was measured (J_{wi}). Then, the feed tank was refilled with a 0.1g/L BSA solution and the permeate flux was obtained (J_p) to investigate the value of the flux reduction. After 2 h filtration of BSA, deionized water was used to wash the membrane surface for 10 min and then pure water flux of the cleaned thin layers was measured (J_{wc}), again. To obtain the antifouling ability of the membranes, the flux recovery ratio (FRR) was calculated using equation (2) [16]:

$$FRR = \left(\frac{J_{wc}}{J_{wi}} \right) \times 100 \quad (2)$$

3. Results and discussion

3.1. Flux and rejection investigation

The flux and rejection capabilities of the prepared membranes were investigated to find the effects of the presence of STPP salt on the performances of the membranes' thin layer. As could be observed in Figure 2, the flux of the unmodified thin layer (M_0) is about 34 LMH ($L/m^2 h$) which is sharply increased to about 74 LMH in the M_1 membrane (composed of 1% w/w STPP). This was about two orders of magnitude higher than that of the

unmodified thin layer. By increasing the STPP concentration to 3 and 5% w/w, the permeate fluxes are decreased to about 60 and 55 LMH, respectively. On the other hand, the STTP-modified thin layers showed an increase in the rejection capability against the Cu^{2+} solution. Accordingly, the rejection of the M_0 thin layer was about 55%. In contrary, all STTP-modified thin layers showed higher rejection against the Cu^{2+} compared to those of the M_0 thin layer without the STTP. The rejection capabilities of M_1 , M_3 , and M_5 were about 70, 72, and 76%, respectively.

3.2. EDX analysis

Before the explanation of the reasons for these alterations, the EDX elemental map of the surface of the prepared membranes is shown. As can obviously be observed in Figure 3, green points correspond to the oxygen atoms in the membranes' structure. These images clearly show that the STPP salts were completely spread within the structure of the prepared thin layers. The percentage value of the oxygen atoms (PVO) is summarized in Table 2.

Table 2. The oxygen percentage and water contact angle of the prepared thin layers.

Membrane	Oxygen (% w/w)	Contact angle (°)
M_s	20.17	-
M_0	18.54	53 ± 3
M_1	27.80	30 ± 2
M_3	31.81	40 ± 3
M_5	41.23	34 ± 3

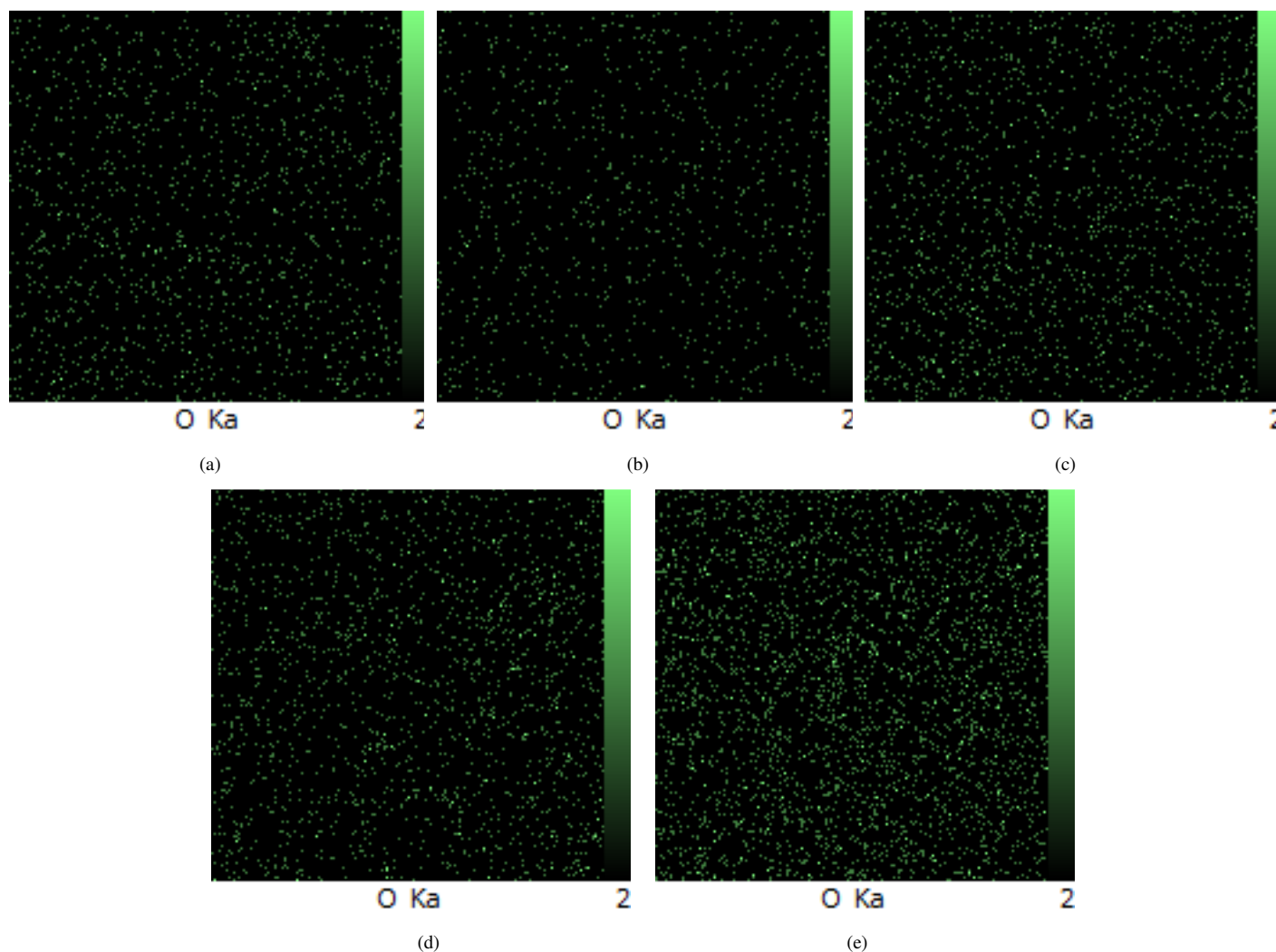


Fig. 3. Surface oxygen elemental analysis of the thin layers using EDX: (a) M_s , (b) M_0 , (c) M_1 , (d) M_3 , and (e) M_5 .

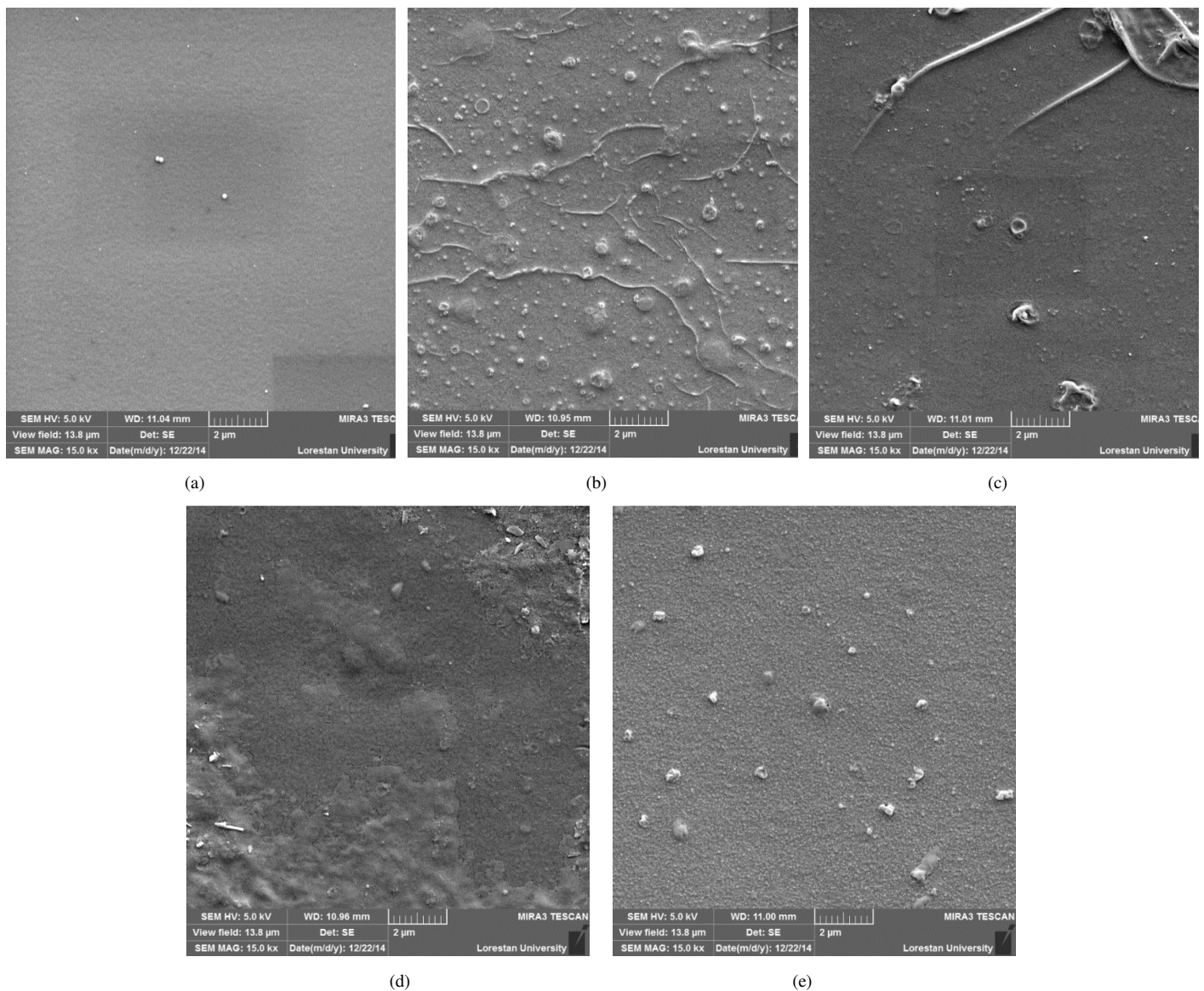


Fig. 4. SEM surface images of the prepared thin layers: (a) M_s , (b) M_0 , (c) M_1 , (d) M_3 , and (e) M_5 .

The PES support (M_s) shows PVO values about 20.17% while those values for M_0 , M_1 , M_3 , and M_5 were about 18.54, 27.80, 31.81, and 41.23%, respectively. These results clearly demonstrated that the STPP salt was remained and captured into the structure of the STPP-modified thin layers. The difference in PVO values of M_s and M_0 was due to different natures of the PES and PA polymers. It seems that in the presence of the STPP salt, the interfacial tension between the aqueous and the organic phases may change. This results in a relative change in the mass transfer of PIP into the organic phase [17]. Furthermore, the STPP contains negative-charged oxygen in its structure which presumably can promote the neutralization of the acid produced during the interfacial polymerization reaction, resulting in further promotion of polymerization [18]. Accordingly, the formation of a dense and compact surface is expected. This phenomenon was compatible with the rejection results of the prepared thin layers. Formation of a more compact thin layer along with the presence of oxygen atoms in the body of the modified thin layer probably increased the rejection ability of the thin layers.

3.3. SEM images

Figure 4 shows the surface structure of the membranes in the absence and presence of the STPP salt. As we can see, the surface structures of the STPP-modified thin layers (Figure 4c-f) were completely different from the unmodified thin layer (Figure 4b). In these images the formation of a dense and compact thin layer on the surface of the membranes is clearly proven. Figure 4c clearly shows that at high STPP concentrations a very dense surface along with an uneven and rough figure including a nodular structure was seen.

However, M_1 membrane (including 1% w/w of STPP) showed high flux (74LMH) and desired rejection (70 %).

As mentioned above, the presence of STPP increased the compactness of the thin layers. In contrary, high flux was observed for M_1 thin layer. This was due to more hydrophilicity of M_1 thin layer. The contact angle values of all thin layers are summarized in Table 2. As is clearly seen, the contact angle values of the STPP-modified thin layers are notably lower than that of the unmodified thin layer (the control sample). The unmodified thin layer showed a contact angle of about 53° while the contact angles of the STPP-modified M_1 , M_3 , and M_5 thin layers are decreased to as low as 30° , 40° , and 34° , respectively. According to obtained results, probably two parameters of hydrophilicity and compactness were competing in the modified thin layers. At low concentrations of STPP, the presence of salt changed the polymerization conditions to create a denser thin layer, but the presence of inorganic salt further increased the hydrophilicity. In higher concentrations, the compactness of the thin layer was more dominant. Accordingly, the flux was decreased while the rejection was increased. The lower contact angle of the M_5 thin layer may be attributed to the high concentration of STPP along with high surface roughness which can increase the specific area of the surface.

3.4. Antifouling properties

During 2 h filtration test of the BSA solution, the flux behavior for prepared thin layers were investigated and the results are diagrammatically shown in Figure 5. For this purpose, the flux recovery ratios (FRR) of the thin

layer membranes were measured to estimate and investigate the antifouling capability of the prepared thin layers. According to the obtained results, the unmodified thin layer showed lower FRR compared to the STPP-modified thin layers. The FRR of the unmodified thin layer was obtained to be about 70% which was increased to as high as 90% in M_1 thin layer. Changing the hydrophilicity and compactness of the thin layer presumably increased the antifouling properties of the STPP-modified thin layers. In these cases, compactness and pore size reduction of the thin layer prevent the diffusion of the foulants into the membranes' structure [19]. Relative decrease in FRR was attributed to the high roughness parameters of the surface and relative increase in hydrophobicity of M_3 and M_5 thin layers.

For this purpose, AFM images were analyzed to investigate the surface nanostructure of the prepared thin layers. These images clearly demonstrated that the roughness parameters of the surface of the STPP-modified thin layers were notably increased.

The thin layers containing high STPP concentrations showed less antifouling properties than that containing lower STPP. It can be concluded that it was due to high surface roughness of the thin layers containing higher salt concentrations (STPP). As known, increasing the roughness parameters decreased the antifouling properties of the surfaces [20].

Regarding the AFM images reinforced by the SPM DME software, there are obvious changes in roughness parameters. Two and three dimensional surface AFM images were obtained for M_0 (Figure 6a) and the STPP-modified thin layers containing 1 (M_1 , Figure 6b), 3 (M_3 , Figure 6c), and 5% w/w STPP (M_5 , Figure 6d) which were studied at a scan size of $3 \times 3 \mu\text{m}$. The surface roughness parameters of the membranes which were explained in terms of

mean roughness (S_a), root mean square of the Z data (S_q), and mean difference between the highest peaks and the lowest valleys (S_z) were measured by SPM DME software and are shown in Table 3.

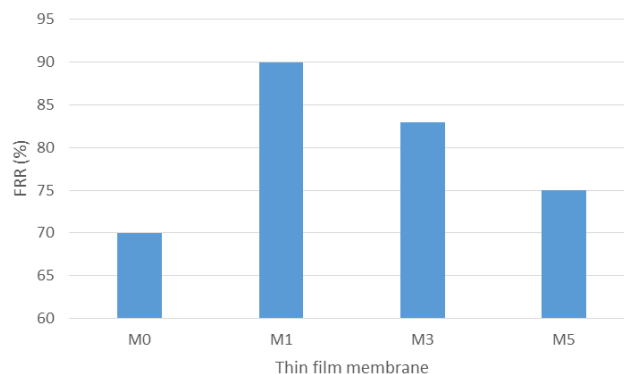


Fig. 5. The FRR values belonged to the thin layers.

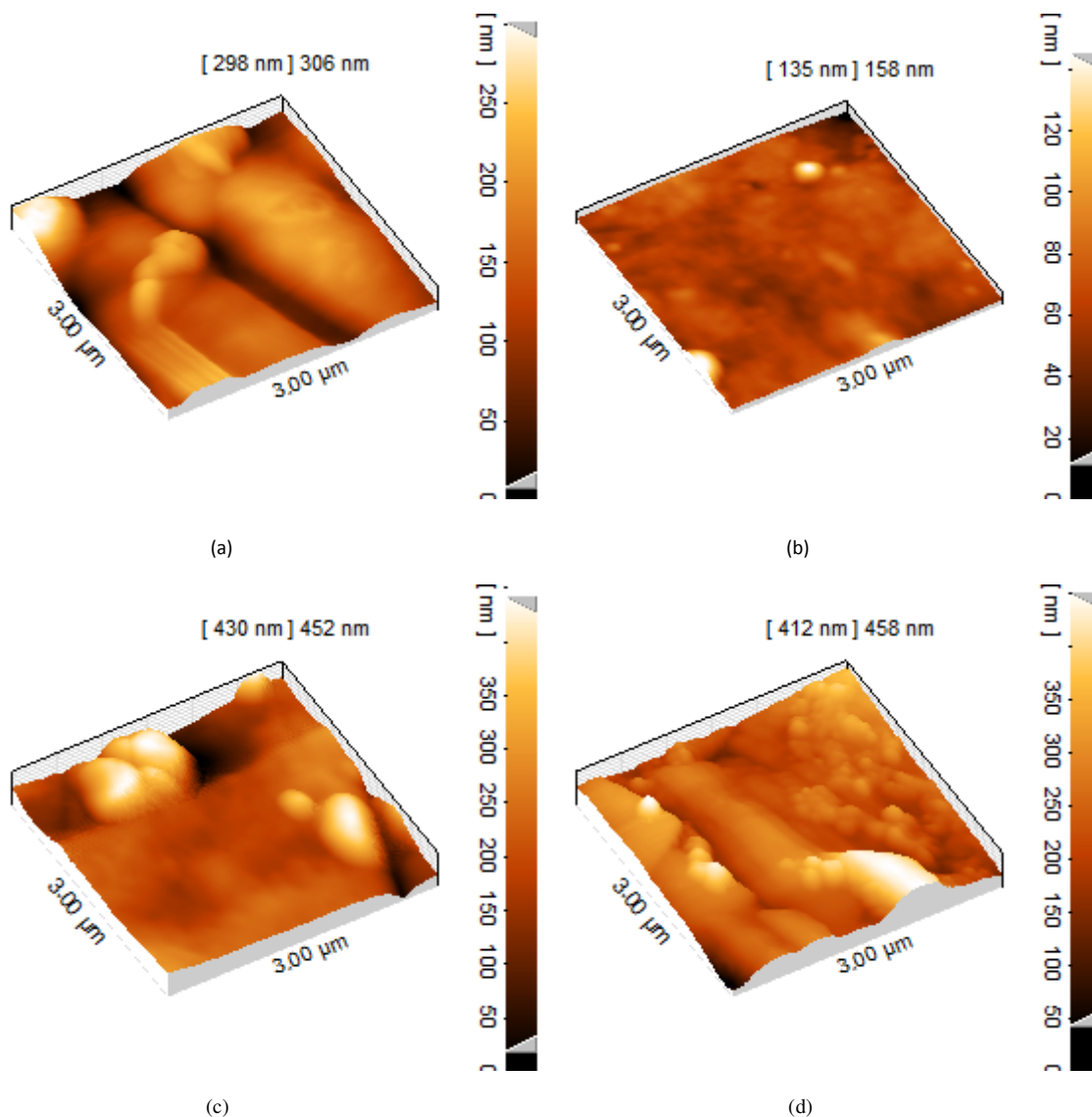


Fig. 6. The AFM images of (a) M_0 , (b) M_1 , (c) M_3 , and (d) M_5 .

As shown in Table 2, M₁ membrane including 1% w/w STPP illustrated the lowest value of roughness among the STPP-modified thin layers. The parameters of S_z, S_a, and S_q for the unmodified thin layer (M₀) were measured at 287, 41.5, and 52.4 nm which were decreased to 65.7, 8.16, and 12.0 nm, respectively. These parameters were obtained to be about 440, 53.6, and 74.2 nm for M₃ membrane and nearly 327, 46, and 62 nm for M₅ membrane, respectively. The smooth surface of M₁ along with the desirable hydrophilicity could increase the thin layer surface power against the settlement of the foulants on the surface. As mentioned above, the ability of the other modified thin layers to avoid settlement of foulants was decreased due to relative increase of the roughness parameters of the surfaces.

Table 3. The roughness parameters calculated with SPM software attached to AFM images.

Membrane	Roughness parameters (nm)		
	S _z	S _a	S _q
M ₀	287	41.5	52.4
M ₁	65.7	8.16	12.0
M ₃	440	53.6	74.2
M ₅	327	46.0	62.0

4. Conclusion

In this work, STPP was used as an inorganic salt to investigate the presence of the salt on the properties and performance of the thin film composite membranes. Increasing the STPP concentration increased the Cu⁺² rejection capability of the membranes from ~50% to higher than 70%. It also increased the flux recovery ratio properties of the membranes from 70% to about 90% for 1 wt%-modified thin layer. Despite high rejection of the prepared thin layers in the highest concentration of STPP, the thin layer membranes including the lowest concentration showed desirable performance due to relatively high rejection as well as the highest flux recovery ratio and the highest flux.

5. Nomenclatures

AFM	Atomic force microscopy
AA	Acrylic acid
ATR	Attenuated total reflection
BSA	Bovine serum albumin (BSA)
EDA	Ethylenediamine
FRR	Flux recovery ratio
IP	Interfacial polymerization
R _{ir}	Irreversible resistance
LMH	L m ⁻² h ⁻¹
NF	Nanofiltration
DMF	N,N-dimethylformamide
PVO	Percentage value of oxygen atoms
PES	Polyethersulphone
PIP	Piperazine
PA	Polyamide
PEG600	Poly (ethylene glycol) 600
R _r	Reversible resistance
SEM	Scanning electron microscopy
TEA	Triethylamine
TMC	Trimesoyl chloride
UF	Ultrafiltration

6. References

- [1] L.P. Raman, M. Cheryan, N. Rajagopalan, Consider nanofiltration for membrane separations, (United State), Chem. Eng. Prog. 90 (1994) 68.
- [2] Y. Mansourpanah, S.S. Madaeni, A. Rahimpour, Fabrication and development of interfacial polymerized thin-film composite nanofiltration membrane using different surfactants in organic phase; study of morphology and performance, J. Membr. Sci. 343 (2009) 219-228.
- [3] X. Wei, X. Kong, J. Yang, G. Zhang, J. Chen, J. Wang, Structure influence of hyperbranched polyester on structure and properties of synthesized nanofiltration membranes, J. Membr. Sci. 440 (2013) 67-76.
- [4] N.K. Saha, S.V. Joshi, Performance evaluation of thin film composite polyamide nanofiltration membrane with variation in monomer type, J. Membr. Sci. 342 (2009) 60-69.

- [5] H. Zhu, A. Szymczyk, B. Balanec, On the salt rejection properties of nanofiltration polyamide membranes formed by interfacial polymerization, J. Membr. Sci. 379 (2011) 215-223.
- [6] S. Yu, M. Ma, J. Liu, J. Tao, M. Liu, C. Gao, Study on polyamide thin-film composite nanofiltration membrane by interfacial polymerization of polyvinylamine (PVAm) and isophthaloyl chloride (IPC), J. Membr. Sci. 379 (2011) 164-173.
- [7] Y. Zhang, Y. Su, Wenjuan Chen, J. Peng, Y. Dong, Z. Jiang, H. Liu, Appearance of poly(ethylene oxide) segments in the polyamide layer for antifouling nanofiltration membranes, J. Membr. Sci. 382 (2011) 300-307.
- [8] V. Freger, Nanoscale heterogeneity of polyamide membranes formed by interfacial polymerization, Langmuir 19 (2003) 4791-4797.
- [9] Y. Mansourpanah, S.S. Madaeni, A. Rahimpour, Z. Kheirollahi, M. Adeli, Changing the performance and morphology of polyethersulfone/polyimide blend nanofiltration membranes using trimethylamine, Desalination 256 (2010) 101-107.
- [10] L. Jin, W. Shi, S. Yu, X. Yi, N. Sun, C. Ma, Y. Liu, Preparation and characterization of a novel PA-SiO₂ nanofiltration membrane for raw water treatment, Desalination 298 (2012) 34-41.
- [11] Y. Mansourpanah, E. Momeni Habili, Investigation and characterization of TiO₂-TFC nanocomposite membranes; membrane preparation and UV studies, J. Membr. Sci. Res. 1 (2015) 26-33.
- [12] K. N. Han, B. Y. Yu, S-Y Kwak, Hyperbranched poly(amidoamine)/polysulfone composite membranes for Cd(II) removal from water, J. Membr. Sci. 396 (2012) 83-91.
- [13] H. Yoo, S.Y. Kwak, Surface functionalization of PTFE membranes with hyperbranched poly(amidoamine) for the removal of Cu²⁺ ions from aqueous solution, J. Membr. Sci. 448 (2013) 125-134.
- [14] A. Sarkar, P.I. Carver, T. Zhang, A. Merrington, K.J. Bruza, J.L. Rousseau, S.E. Keinath, P.R. Dvornic, Dendrimer-based coatings for surface modification of polyamide reverse osmosis membranes, J. Membr. Sci. 349 (2010) 421-428.
- [15] M. L. Lind, A. K. Ghosh, A. Jawor, X. Huang, W. Hou, Y. Yang, E. M. V. Hoek, Influence of zeolite crystal size on zeolite-polyamide thin film nanocomposite membranes, Langmuir, 25 (2009) 10139-10145.
- [16] J. Peng, Y. Su, Q. Shi, W. Chen, Z. Jiang, Protein fouling resistant membrane prepared by amphiphilic pegylated polyethersulfone, Bioresource Technol. 102 (2011) 2289-2295.
- [17] Y. Mansourpanah, Z. Jafari, Efficacy of different generations and concentrations of PAMAM-NH₂ on the performance and structure of TFC membranes, React. Func. Polym. 93 (2015) 178-189.
- [18] S. Yu, M. Ma, J. Liu, J. Tao, M. Liu, C. Gao, Study on polyamide thin-film composite nanofiltration membrane by interfacial polymerization of polyvinylamine (PVAm) and isophthaloyl chloride (IPC), J. Membr. Sci. 379 (2011) 164-173.
- [19] J. Luo, S.T. Jianquan, A.S. Meyer, M. Pinelo, Filtration behavior of casein glycomacropptide (CGMP) in an enzymatic membrane reactor: fouling control by membrane selection and threshold flux operation, J. Membr. Sci. 469 (2014) 127-139.
- [20] E.M. Vrijenhoek, S. Hong, M. Elimelech, Influence of membrane surface properties on initial rate of colloidal fouling of reverse osmosis and nanofiltration membranes, J. Membr. Sci. 188 (2001) 115-128.